

Performance enhancement of maximum power point tracking for grid-connected photovoltaic system under various gradient of irradiance changes

Mario Norman Syah^{*1}, Subiyanto²

¹Electrical Engineering Department, SMK N 1 Blado, Kalipancur St. 51255, Blado, Batang, Indonesia

²Electrical Engineering Department, Universitas Negeri Semarang,
Office E11, Sekaran Campus 50229, Semarang, Indonesia

*Corresponding author, e-mail: marionorman@students.unnes.ac.id¹, subiyanto@mail.unnes.ac.id²

Abstract

This paper presents a new variant of smart adaptive algorithm of Maximum Power Point Tracking (MPPT) in the photovoltaic (PV) system. The algorithm was adopted from Modified Perturb and Observe (MP&O). The smart adaptive MPPT is used to search Maximum Power Point (MPP) of the PV system under various irradiance changes. This algorithm incorporates information of current change (ΔI), maximum operating point margin and dynamic perturbation step to prevent MPPT diverging away from the MPP and minimize the steady state oscillation. The smart adaptive MPPT algorithm performance is compared with the dl-P&O and conventional P&O to prove its effectiveness. The comparison is performed under the various gradient of irradiance change. It was found that, for all the tests, the smart adaptive algorithm scheme improve the tracking efficiency under various gradients of irradiance changes and increase the efficiency of extraction power from PV system.

Keywords: *perturb and observe, photovoltaic system, PSIM, smart adaptive*

Copyright © 2019 Universitas Ahmad Dahlan. All rights reserved.

1. Introduction

Renewable energy generation growth has been increasing quickly due to the continuous reduction of fossil fuel energy generation [1]. The photovoltaic (PV) generation increasing 267.1 GW in the past 4 years [2]. Solar is a viable alternative energy resource. Solar energy is becoming important as a renewable energy resource. Consequently, It gives great merits such as simple of installation, less maintenance, and no pollutions [3]. PV generation is possible to substitute fossil energy generation. The grid-connected PV system is more advantageous in terms of cost and investment than the standalone PV system [4].

PV module conversion efficiency leans on the operating point on the characteristic curve of the PV module that is not linear and influenced by solar irradiances and ambient temperature [5]. There is maximum power point (MPP) at each characteristic curve of the PV module. In order to make the PV generation system operate at its maximum power, MPPT is employed [6]. MPPT is the main function that should include in every PV system to ensure that PV system generates possible maximum power [7]. Since the MPPT is ordinarily areas to improve the effectiveness of PV conversion because it consists of software codes that can embed into the microcontroller and is the most economical method for increasing the maximum energy of a PV system [7, 8]. The existing algorithms of MPPT include the voltage feedback method [9,10], the current feedback method [11, 12], the incremental conduction (INC) method, perturb and observe (P&O) method [13, 14], artificial neural network (ANN) method [15, 16], fuzzy logic methods [17, 18].

The most used MPPT techniques are P&O and INC due to their simplified algorithm control and low-cost implementation. INC method is better than P&O because it based on the derivative of PV module output power with its voltage. Moreover, Compared INC method and P&O method show that INC has many advantages in the tracking speed, tracking accuracy and efficiency [19]. Besides that, P&O method is simpler than INC method in practical applications. The algorithm operation is adversely affected by noise and errors on the measured control values [20]. The P&O has two serious drawbacks. The first is oscillation around the MPP when steady state. Second is the false perturbation step when rapid change of irradiance.

The both drawbacks reduced the efficiency of output power and tracking efficiency. Many researchers have developed the MPPT techniques to minimize these two drawbacks. Adding PV module current (I_{pv}) as controlled variable is to resolve the false perturbation issue [21]. However, the developed techniques are just for specific conditions. This technique only works when the algorithm deviated to the right of the P-V curve. There are other developed adaptive techniques to solve these drawbacks. The developed techniques exhibits high performance and solve both drawbacks. However, it needs the complex computational and make it difficult to implement. Another issue is the MPPT algorithms performance benchmarking is tested on simple G profiles [22]. It does not reflect the real environmental conditions. Authors in [23] have developed A Modified P&O to find the MPP and improved tracking efficiency. But, the performance of the MPPT PV system under the various gradient of irradiance changes conditions need to be developed and evaluated.

In this work, a new variant of smart adaptive algorithm for MPPT PV system based on Modified P&O [23] was developed and evaluated in the various conditions. The algorithm has additional structures that incorporates information of current change, maximum operating point margin and dynamic perturbation step to avoid MPPT from losing of tracking direction and to reduce steady-state oscillation under various conditions. The smart adaptive MPPT are simulated using PSIM and comprehensively benchmarked using MPPT efficiency test. This test order the algorithm to track various gradient G profile. Results show the compared performances of the developed MPPT algorithm and conventional MPPT algorithms.

2. Developed System Model

2.1. Photovoltaic Module Modeling

The fundamental component in PV module is a PV cell. The output of a PV cell is very low. In order to meet practical demands, they are connected in series (N_s) or in parallel (N_p) or in series-parallel [23] as shown in Figure 1. V_{pv} is the PV cell voltage and $N=N_s/N_p$, the current I can be written as:

$$I = I_{PV}N_p - I_{D1} - I_{D2} - \frac{V+NIR_s}{NR_p} \quad (1)$$

$$I_{D1} = I_{d1}N_p \left[\exp\left(\frac{V+NIR_s}{a_1V_{T1}N_s}\right) \right] \quad (2)$$

$$I_{D2} = I_{d2}N_p \left[\exp\left(\frac{V+NIR_s}{a_2V_{T2}N_s}\right) \right] \quad (3)$$

where I is the current and V is the voltage. R_s and R_p is the series resistance, and R_p is the parallel resistance, while $V_{T1} = V_{T2}$ is the thermal voltage of the diodes and $a_1 = a_2$ is the ideality factor of the diode. I_{PV} is the light generated current which given by

$$I_{PV} = (I_{PV_{STC}} + K_1(T - T_{STC})) \frac{G}{G_{STC}} \quad (4)$$

where G is the irradiance and T is temperature. Note that $I_{PV_{STC}}$, G_{STC} , and T_{STC} are that measured in the standard test condition (STC). K_1 is short circuit current coefficient. $I_{d1} = I_{d2}$ is the diode saturation current. It is written as:

$$I_{d1} = I_{d2} = \frac{I_{sc} + K(T - T_{STC})}{\exp((V_{oc} + K_v(T - T_{STC}))/V_T)} - 1 \quad (5)$$

According to (5), I_{sc} is short circuit current in STC and V_{oc} is the open circuit voltage in STC. K_v is the temperature coefficient of the voltage. In this study, we use JA Solar Cell JAP6 60-250 3BB panel. The JA Solar Cell JAP6 60-250 3BB panel is modeled using PSIM physical model of PV module by entering basic parameter from its datasheet as shown in Table 1. The JA Solar Cell JAP6 60-250 3BB is modeled using PSIM software.

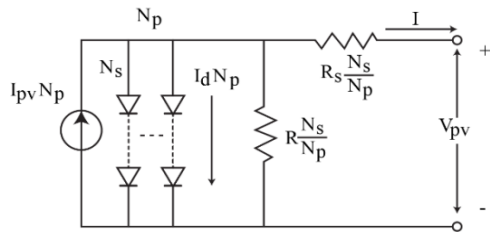


Figure 1. The equivalent circuit of two-diode PV cell

Table 1. The Specification of the PV Module (JAP6 60-250)

Parameters	Label	Value
Short Circuit Current	I_{SC}	8.92 A
Open Circuit Voltage	V_{OC}	37.66 V
Current at Pmax	I_{MPP}	8.35 A
Voltage at Pmax	V_{MPP}	29.94 V
Maximum Power	P_{MPP}	250 W
Voc coef. of temperature	K_V	-0.3308 % /°C
Isc coef. of temperature	K_I	0.058 % /°C
Cell in series per module	N	60

2.2. Design of Grid-Connected PV System

In The grid-connected PV system is simulated to test the MPPT method. The system consist of PV module array, DC/DC Boost Converter, inverter, L filter, grid, and load as shows in Figure 2.

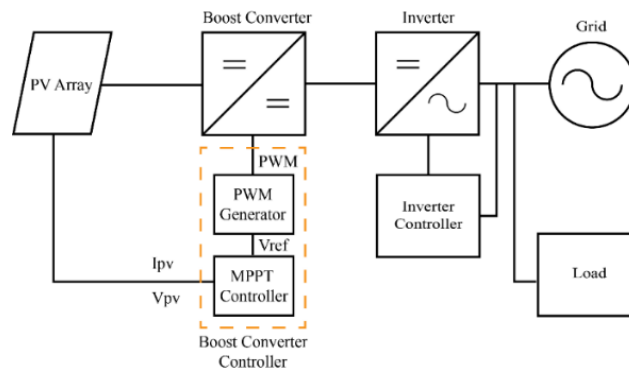


Figure 2. Block diagram of grid-connected photovoltaic system

3. MPPT Algorithm

Many MPPT methods have been implemented in PV power plants. The P&O is the most popular to solve the efficiency problems of PV power generation. These methods are still developed to increase its performance.

3.1. Conventional Perturb and Observe (P&O)

This algorithm is the most popular in practice because of its simple control algorithm. However, it is not powerful enough to track the right MPP when rapid irradiance change [15, 22, 23]. This algorithm searches MPP by changing the operating point with the perturbation step (ΔC) and then the change in P (ΔP) is measured. The formulation for changing operation point can be expressed as follows:

$$C_{new} = C_{old} + \Delta C \phi \tag{6}$$

The algorithm use controlled variable (C) and it can be either voltage (V), current (I) or duty cycle (d). C_{new} and C_{old} is the controlled variable at k and k-1 iteration, respectively. The perturbation step (ΔC) can be Δd , ΔV or ΔI according to the controlled variable that algorithm used. The direction of perturbation is indicated by multiplier *slope*: +1 or -1. They are increasing and decreasing controlled value (C). If $\Delta P > 0$, then the multiplier *slope* keep on its value until the algorithm reaches MPP. Once the $\Delta P < 0$, the multiplier *slope* goes to the opposite direction and the algorithm climbs the P-V curve until reaches the MPP again. It causes the operation point moves back and forth around the MPP. The perturbation step value (ΔC) is vital. If ΔC is small, it results in small oscillation. Consequently, the algorithm response is slow and vice versa [23]. The flow diagram of P&O shown in Figure 3.

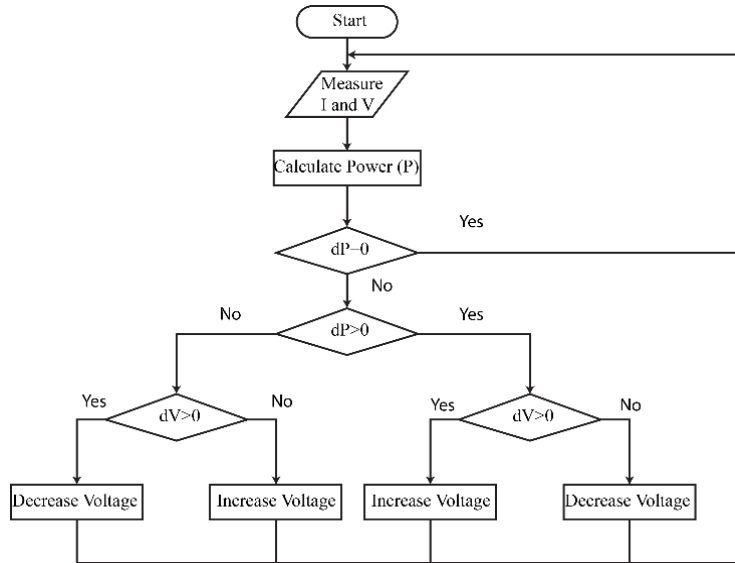


Figure 3. Flowchart of conventional perturb and observe algorithm

3.2. di-P&O

The di-P&O MPPT algorithm adds information of current change (ΔI) to eliminate the conventional P&O problems [21]. The relation between the current and voltage corresponding the present operating point on $I-V$ characteristics of the PV module shown Figure 4 (a). As shown in Figure 4 (a) suppose there is an increase in irradiation while the operating point at C, then the operating point will reach to a new point D in the new irradiance curve. Then algorithm makes a decision when $\Delta I > 0$ at operating point D. At the same time, both $\Delta P > 0$ and $\Delta V > 0$ on the $P-V$ characteristics at point D, as shown in Figure 4 (b). Thus, ΔP , ΔV , and ΔI are positive at point D as shown in Figure 4 (a) and Figure 4 (b). Thus, the additional parameter ΔI can detect the positive value of ΔP is due to increase in irradiation and thereby decreasing the operating voltage where both $\Delta V > 0$ and $\Delta I > 0$ can eliminate the drift problem by moving the operating point closer to the MPP as shown in Figure 4 (b). The flow diagram of di-P&O shown in Figure 5.

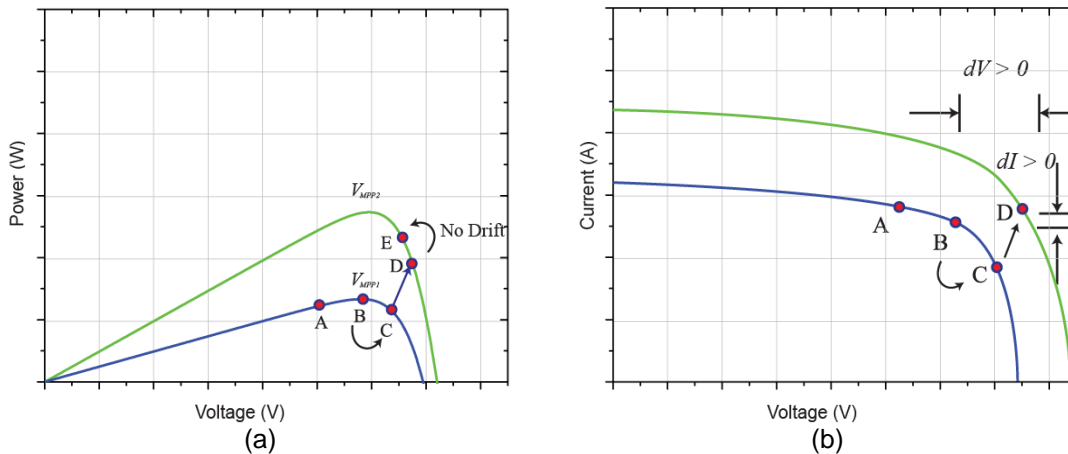


Figure 4. (a) Current and voltage relation of PV (b) tracking process of di-P&O

4. Smart Adaptive MPPT Algorithm

The new variant of smart adaptive MPPT algorithm is developed to minimize the steady state oscillation and avoid MPP tracking deviation. The algorithm starts by taking a few

perturbations to track uniform of G . The oscillation around MPP take effect after algorithm reaching the operating point near the MPP. The oscillation is detected by collecting the multiplier values of algorithm move on the P-V curve, i.e. ΔP , ΔV and ΔI when it searches the MPP. During the increasing or decreasing of the voltage, *slope* value could be either positive or negative. These values is the sign multiplication of ΔP , ΔV , and ΔI . They will be used to determine whether the algorithm has converged to MPP and hence variations in the step value of the perturbation. This procedure is possible to detect the occurrence of oscillation precisely. Once it detected, the initial perturbation step value (2% of V_{oc_array}) is reduced 0.5% of V_{oc_array} in every iteration until its reaches minimum value (0.5% of V_{oc_array}) to resolve the problem of oscillation.

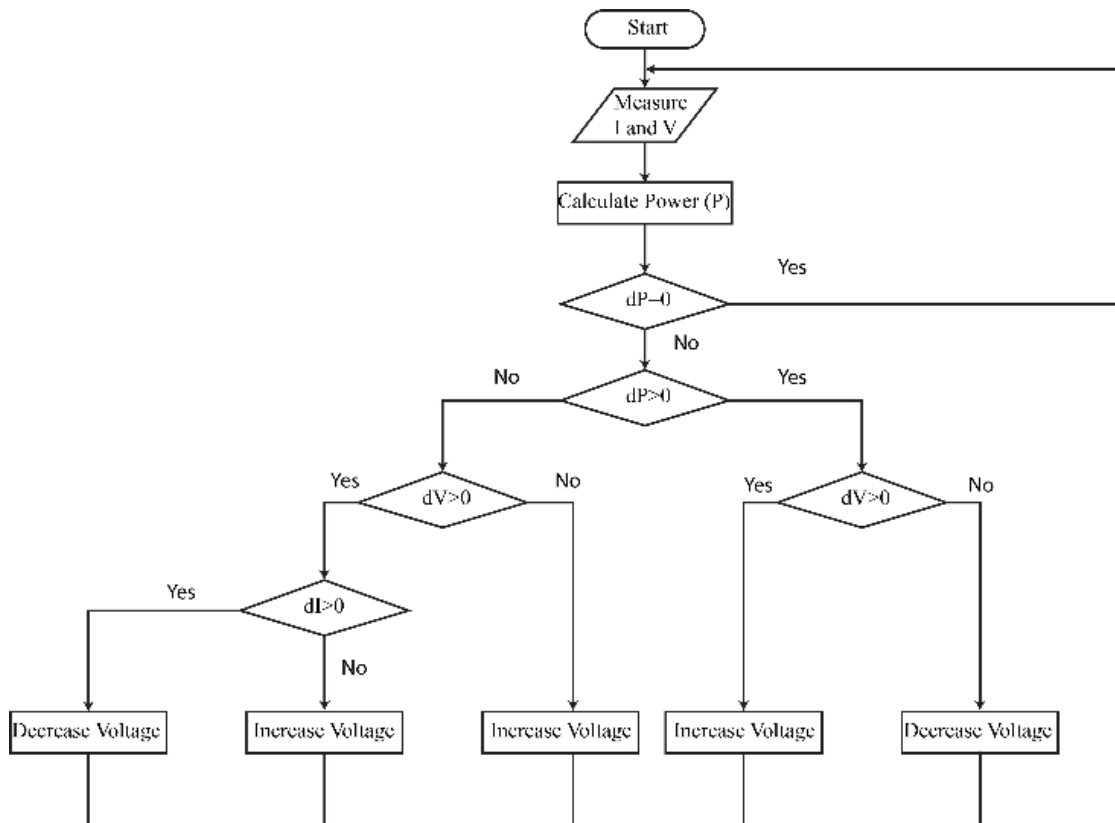


Figure 5. Flowchart of dI-P&O algorithm

This algorithm avoid possible false tracking direction that conventional P&O is still suffering. Ordinarily, in the real environment the conventional P&O treat equally the variation of G with fixed perturbation step. When G changes slowly, the conventional P&O can cope with these changes. However, when fast increasing of G , the conventional P&O likely suffer from loss of tracking direction. The following procedure needs the value of irradiance change, but the method does not require irradiance sensor to measure the change of G . The MPPT takes consecutive sampling when irradiance starts changing. It is assumed that T will remain almost the same value. If T remains constant in two consecutive samples, the relationship of the samples as given by [23].

From [23] can be concluded that the normalized power change is equivalent to the normalized irradiance change. In this simulation, the minimum change in power ($\Delta P/P$) is set to be 0.0002 based on trial and error observation from simulation as do as in [24]. This value selected as the as the threshold ΔTr . If the $\Delta P/P \geq \Delta Tr$, the perturbation step value is returned to the initial value to track the MPP. Elseways, it kept to the minimum value. In some case, the MPP voltage will decrease when level of irradiance is high due to the panel series

resistance [25] and it causing PV power is decrease and high change in power is raise. This threshold can solve the problem caused by that situation.

The mechanism how the algorithm minimizes the possible false of MPPT direction shown in Figure 6. In order to eliminate this problem, the voltage margin is imposed once steady-state oscillation is detected. Initial voltage margin is set to 0.5 % of Open circuit voltage (V_{oc}) to 0.95 % V_{oc_array} at the beginning, $V_{oc_array} = V_{oc} \times N_s$. When the steady-state oscillation detected, the voltage margin change to $V_{mpp} - 0.05 V_{oc_array}$ to $V_{mpp} + 0.05 V_{oc_array}$. Note that V_{mpp} is the target Voltage of MPP. When G increases, the V_{mpp} actually shifts 5 % of V_{oc_array} to the right. The operating point is restricted to 5 % of V_{oc_array} margin to force the operating point always close the MPP. This procedure can avoid the loss of tracking. The flow diagram of smart adaptive MPPT algorithm is presented in Figure 7.

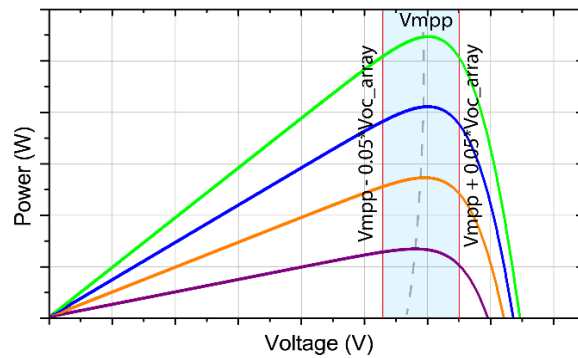


Figure 6. The margin of VMPP

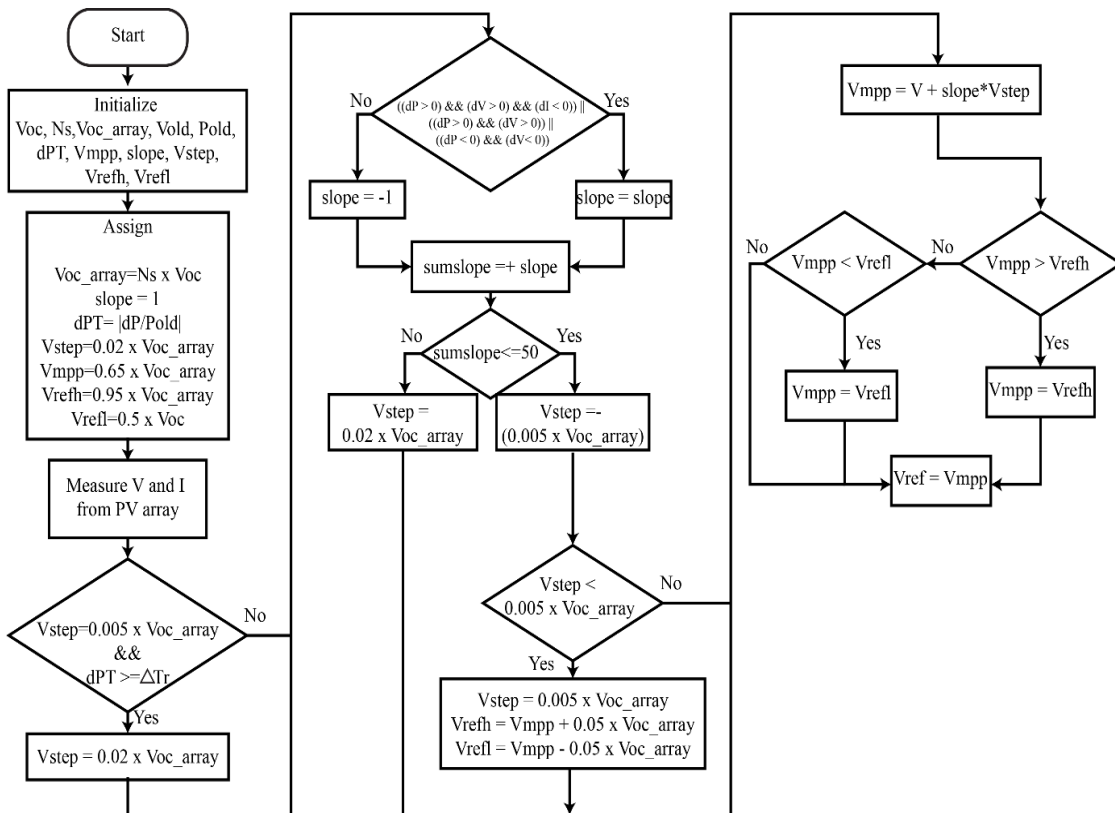


Figure 7. Flowchart of smart adaptive MPPT algorithm


```

{
  //SMART ADAPTIVE MPPT ALGORITHM

  //Inisialisasi variabel
  static double Vref=244.79;
  static double Vrefh=357.77;
  static double Vrefl=18.83;
  static double P, Pold, dP, dV, Vpv,dI, dPT, Vmpp, Vstep=7.532;
  static double slope, sumslope, sum;
  static int i, o;
  P=in[0];
  Pold=in[1];
  dP=in[2];
  dV=in[3];
  Vpv=in[4];
  dPT=fabs(in[5]);
  dI=in[6];
}

```

Figure 10. Implementation of smart adaptive MPPT algorithm on C block PSIM

Table 2. PSIM Simulation Parameters

PSIM Simulation Parameters	
Time step	2 μ s
Total time	0.87 s (Standalone) 1.743 s (on grid)
Print time	0.2 s
System parameters	
Voltage source (Vmpp)	330 V – 370 V
Frequency Grid System	50 Hz
Voltage Grid System	380 V
Impedance of Feeder	R=0.1 m Ω , X _L =0.016 mH
Load	P ₁ =5 kW, Q ₁ =2421.62 VA, P ₂ =10 kW, Q ₂ =4843.21 VA, P ₃ =15 kW, Q ₃ =7264.83 VA
DC link voltage	750 V
DC link capacitor	0.173 mF
Switching frequency	15000 Hz
L filter	4.05 mH
L boost	0.188 mH
C1 boost	2.35 mF
C2 boost	0.173 mF

6. Result and Discussion

The PV system consists of 10 modules in series and 6 modules in parallel. Different level of irradiance is applied to modules. The study is to verify response of the MPPT method under the various gradient of irradiance change, as shown in Figure 11. Moreover, the power flow of the PV-grid system is also presented due to different load conditions.

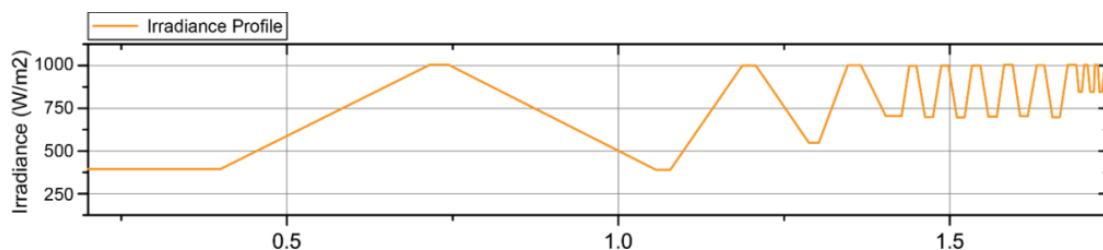


Figure 11. Irradiance profile

Figure 11 shows the irradiance profile to evaluate the capability of smart adaptive MPPT. The algorithm is compared with conventional P&O and dI-P&O. The Smart Adaptive

MPPT works well under various gradient of irradiance change. Moreover, it can be clearly seen that the Smart Adaptive MPPT algorithm can track the MPP almost accurately under various irradiance profile. The performance of the MPPT method is benchmarked using the equations, i.e.

$$\eta_{MPPT} = \frac{P_{out}(t)}{P_{max}(t)} \tag{7}$$

from (7), the average efficiency calculate using

$$\eta_{MPPT} = \frac{\int P_{out}(t)dt}{\int P_{max}(t)dt} \tag{8}$$

From (7), (8), P_{max} is the theoretical maximum power which PV array possible to generate. P_{out} is the extracted power from PV array by the MPPT algorithm. From the simulation, the smart adaptive MPPT can handle the drawbacks of the two MPPT algorithm, i.e. P&O and dl-P&O. The dynamic perturbation step can minimize the oscillation as show in Figure 12, image 1 and image 2. Moreover, image 3 shown the smart adaptive improved the dynamic responses under various change of irradiance. When rapid irradiance changes occur, the conventional P&O and dl-P&O loss their tracking direction as shown in Figure 12, image 4. Their efficiency drops due to this G change. The smart adaptive MPPT is capable to track MPP under various conditions. Consequently, it can track the irradiance gradient locus.

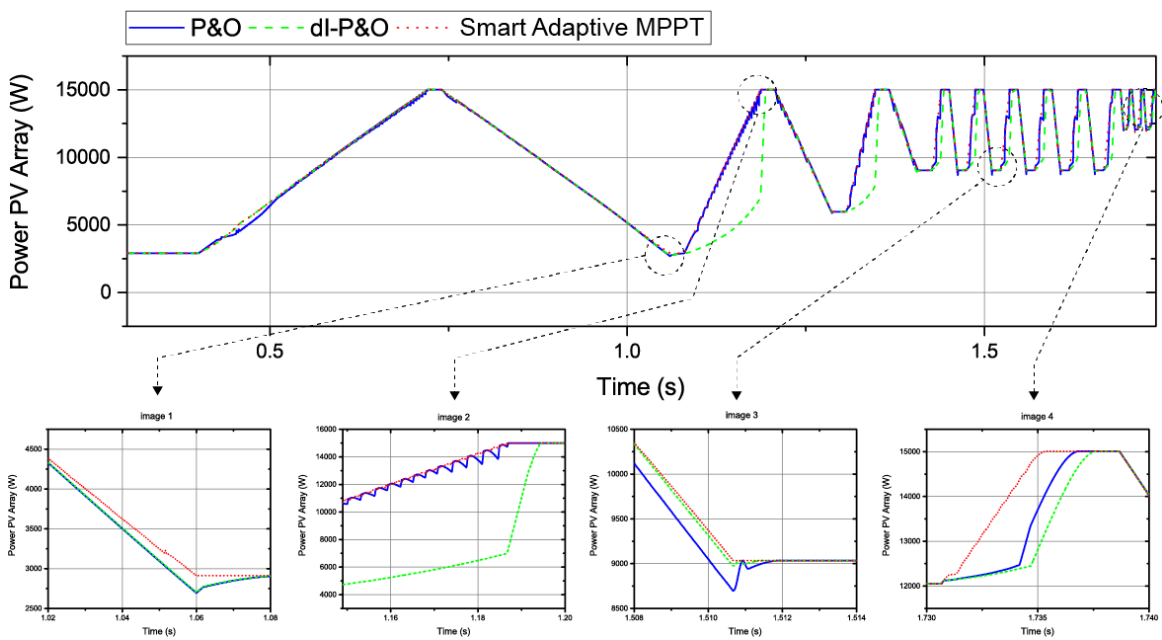


Figure 12. MPPT simulation result

Figure 13 shows the efficiency of MPPT method under various conditions. The graph shows the effect of oscilation and diverging of MPPT tracking. In the rapid change of irradiance at time 1–1.7 s, the conventional P&O and dl-P&O loss their tracking direction as shown in Figure 12. Their efficiency drops due to this irradiance change. It can track follow the irradiance gradient locus.

The deviating can occur towards to the left or to the right of the P-V curve. Figure 14 (a) shows the smart adaptive MPPT performance to track the MPP. Figure 14 (b) shown the V_{mpp} of smart adaptive MPPT is restricted by voltage margins to prevent the voltage diverging away from the V_{mpp} , while the P&O and dl-P&O voltage diverging away from the V_{mpp} . As a result, the efficiency increase and there is not a negligible deviation of power. In some period, power is not

at its P_{mpp} . Ordinarily, this is because of the voltage not exactly on V_{mpp} , and it stays around to the V_{mpp} .

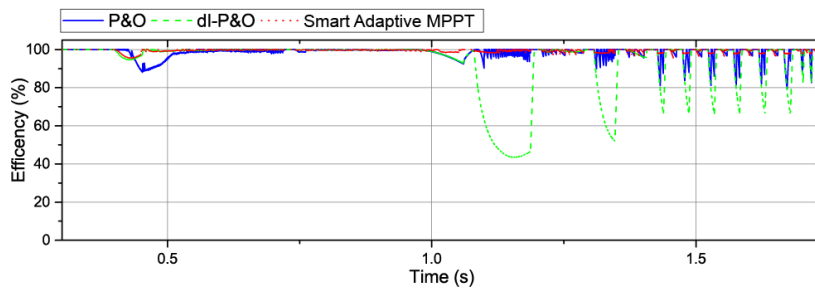


Figure 13. MPPT algorithm efficiency

In grid-connected PV system simulation, the power flow under transient condition is shown in Figure 15. The initial load is 10 kW in time 0–0.3 s and change to 5 kW in time 0.3–0.6 s. In time 0.6–1 s the load increases to 15 kW. PV system supplies 12 kW of power. It can be seen transient load conditions causes changing of power flow.

Figure 15 shows the initial load is 10 kW. Consequently, the PV system is capable of supplying power to the load. The remaining power 2 kW flows into the grid. When the load is 5 kW, PV system can supply 5 kW of power to the load and 7 kW to the grid. When the 12 kW PV power supply the 15 kW load, grid supply the remaining 3 kW of power. It shows that the PV system still supplies 12 kW power to the load. The simulation shows that the PV system is capable during grid-connected condition and transient load condition.

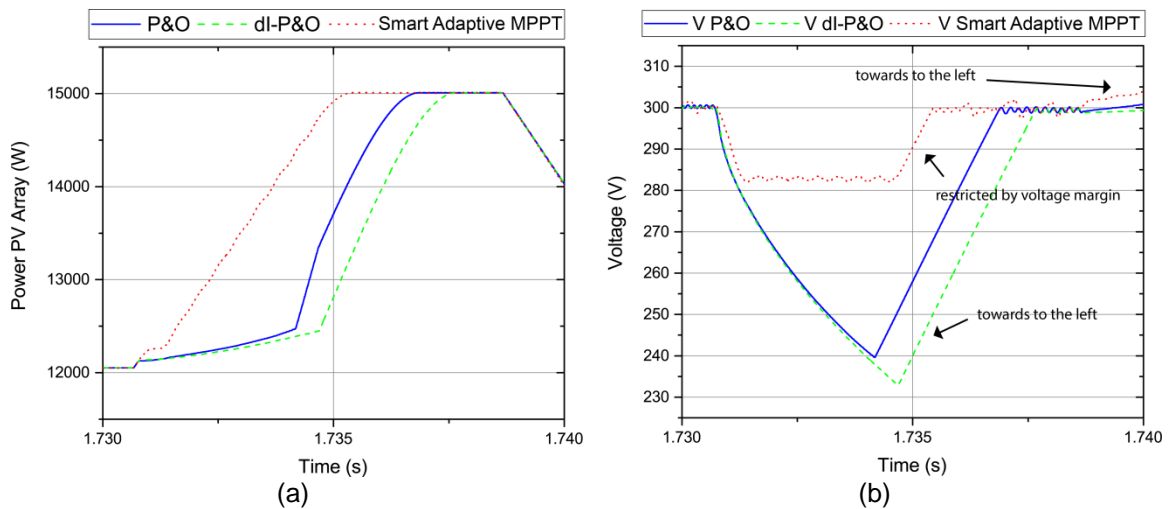


Figure 14. (a) The modified P&O tracking performance (b) Voltage operation of the MPPT

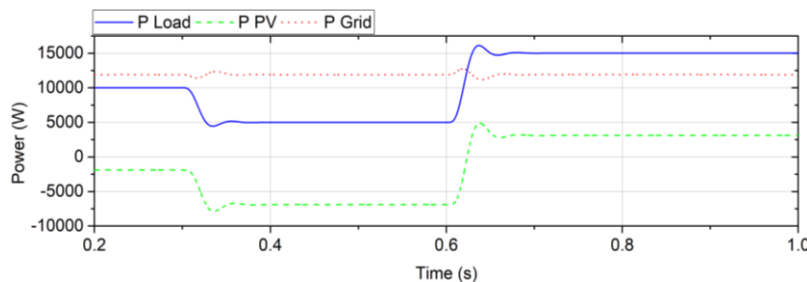


Figure 15. Grid-connected PV system simulation under transient condition

7. Conclusion

In this work, the new smart adaptive MPPT algorithm is implemented to simulate the grid-connected PV system. This algorithm is adapted from modified P&O with adding information of current change (ΔI), maximum operating point margin and dynamic perturbation step. The dl-P&O and Conventional P&O MPPT method are implemented in the system to do performance comparison with new smart adaptive MPPT algorithm and they are tested under various gradients of irradiance changes. As a result, the new smart adaptive MPPT algorithm provides highest efficiency tracking and power conversion compared to the dl-P&O and conventional P&O in the rapid changes of irradiances. In the different load conditions, PV system is capable supplying the power to the load. The power flow from the grid depends on the supply power of the PV system and capacity load.

Acknowledgement

The authors would like to thank Pusat kajian smart clean energy and PUI Hybrid Energy BFSC LPPM Universitas Negeri Semarang, Indonesia, which has supported and facilitated this research. Moreover, gratefully acknowledge UNNES Electrical Engineering Students Research Group (UEESRG) for providing great support to conduct this research work.

References

- [1] Tiku D. *Modular Multilevel MMI(HB) Topology for Single-Stage Grid Connected PV Plant*. 11th IET International Conference on AC and DC Power Transmission. Birmingham. 2015; July: 1–8.
- [2] Mary B (ed.). *Snapshot of global photovoltaic markets*. International Energy Agency (IEA). Report number: T1–31: 2017. 2017
- [3] Liu F, Kang Y, Yu Z, Duan S. *Comparison of P&O and hill climbing MPPT methods for grid-connected PV converter*. 2008 3rd IEEE Conference on Industrial Electronics and Applications. Singapore. 2008; August: 804–807.
- [4] Kouro S, Leon JI, Vinnikov D, Franquelo LG. *Grid-Connected Photovoltaic Systems: An Overview of Recent Research and Emerging PV Converter Technology*. *IEEE Industrial Electronics Magazine*. 2015; 9(1): 47–61.
- [5] Quamruzzaman M, Rahman KM. *A Modified Perturb and Observe Maximum Power Point Tracking Technique for Single-Stage Grid-Connected Photovoltaic Inverter*. *WSEAS Transactions on Power Systems*. 2014; 9: 111–118.
- [6] Mustafa MN. *Design of a Grid Connected Photovoltaic Power Electronic Converter*. Master Thesis. Tromsø: Universitet i Tromsø; 2017.
- [7] Khaled M, Ali H, Abd-El Sattar M, Elbaset AA. *Implementation of a modified perturb and observe maximum power point tracking algorithm for photovoltaic system using an embedded microcontroller*. *IET Renewable Power Generation*. 2016; 10(4): 551–560.
- [8] Hossain MI, Khan SA, Shafiullah M, Hossain MJ. *Design and implementation of MPPT controlled grid connected photovoltaic system*. 2011 IEEE Symposium on Computers & Informatics. 2011: 284–289.
- [9] Chiang W-J, Jou H-L. *Maximum power point tracking method for the voltage-mode grid-connected inverter of photovoltaic generation system*. 2008 IEEE International Conference on Sustainable Energy Technologies. 2008; November: 1–6.
- [10] Veerachary M, Senjyu T, Uezato K. *Voltage-based maximum power point tracking control of PV system*. *IEEE Transactions on Aerospace and Electronic Systems*. 2002; 38(1): 262–270.
- [11] Cha H, Lee S. *Design and Implementation of Photovoltaic Power Conditioning System Using a Current Based Maximum Power Point Tracking*. 2008 IEEE Industry Applications Society Annual Meeting. 2008; October: 1–5.
- [12] Masoum M a. S, Dehbonei H, Fuchs EF. *Theoretical and experimental analyses of photovoltaic systems with voltage and current-based maximum power-point tracking*. *IEEE Transactions on Energy Conversion*. 2002; 17(4): 514–522.
- [13] Putri RI, Wibowo S, Rifa'i M. *Maximum power point tracking for photovoltaic using incremental conductance method*. *Energy Procedia*. 2015; 68: 22–30.
- [14] Sera D, Mathe L, Kerekes T, Spataru SV, Teodorescu R. *On the perturb-and-observe and incremental conductance mppt methods for PV systems*. *IEEE Journal of Photovoltaics*. 2013; 3(3): 1070–1078.
- [15] Elobaid L. *Artificial neural network based maximum power point tracking technique for PV systems*. *IECON 2012-38th*. 2012; October: 937–942.
- [16] Punitha K, Devaraj D, Sakthivel S. *Artificial neural network based modified incremental conductance algorithm for maximum power point tracking in photovoltaic system under partial shading conditions*. *Energy*. 2013; 62: 330–340.

-
- [17] Algazar MM, Al-Monier H, El-Halim HA, Salem MEEK. Maximum power point tracking using fuzzy logic control. *International Journal of Electrical Power & Energy Systems*. 2012; 39(1): 21–28.
- [18] Sharma C, Jain A. Modeling of Buck Converter Models in MPPT using PID and FLC. *TELKOMNIKA Telecommunication Computing Electronics Control*. 2015; 13(4): 1270.
- [19] Jusoh A, Alik R, Guan TK, Sutikno T. MPPT for PV System Based on Variable Step Size P & O Algorithm. *TELKOMNIKA Telecommunication Computing Electronics Control*. 2017; 15(1): 79–92.
- [20] Islam FR, Prakash K, Mamun KA, Lallu A, Mudliar R. Design of an optimum MPPT controller for solar energy system. *Indonesian Journal of Electrical Engineering and Computer Science*. 2016; 2(3): 545–553.
- [21] Killi M, Samanta S. Modified perturb and observe MPPT algorithm for drift avoidance in photovoltaic systems. *IEEE Transactions on Industrial Electronics*. 2015; 62(9): 5549–5559.
- [22] Motahhir S, Ghzizal A El, Sebti S, Derouich A. *Proposal and Implementation of a Novel Perturb and Observe Algorithm using Embedded Software*. 2015 3rd International Renewable and Sustainable Energy Conference (IRSEC). 2015; December: 7–11.
- [23] Ahmed J, Salam Z. A Modified P and O Maximum Power Point Tracking Method with Reduced Steady-State Oscillation and Improved Tracking Efficiency. *IEEE Transactions on Sustainable Energy*. 2016; 7(4): 1506–1515.
- [24] Alqarni M, Darwish MK. *Maximum power point tracking for photovoltaic system: Modified Perturb and Observe algorithm*. 2012 47th International Universities Power Engineering Conference (UPEC). 2012; September: 1-4.
- [25] Scarpa V, Buso S, Spiazzi G. *Low complexity MPPT technique exploiting the effect of the PV cell series resistance*. IEEE Applied Power Electronics Conference and Exhibition. 2008; February: 1958-1964.